The charge density wave and spin density wave in interchain coupled alternate π-conjugated organic ferromagnets

1998 J. Phys.: Condens. Matter 10 1371

(http://iopscience.iop.org/0953-8984/10/6/019)

J. Phys.: Condens. Matter **10** (1998) 1371–1379. Printed in the UK PII: S0953-8984(98)87486-9

The charge density wave and spin density wave in interchain coupled alternate π-conjugated organic ferromagnets

W Z Wang†, K L Yao‡ and H Q Lin§

† Department of Physics, Huazhong University of Science and Technology, Wuhan 430074, People's Republic of China

‡ CCAST (World Laboratory), PO Box 8730, Beijing 100080, People's Republic of China

§ Department of Physics, The Chinese University of Hong Kong, Hong Kong, People's Republic of China

Received 10 September 1997, in final form 27 November 1997

Abstract. Based on a theoretical model proposed for interchain coupled quasi-one-dimensional organic ferromagnets, the distribution of the charge density and spin density are studied. The next-nearest-neighbouring hopping interaction, the strong electron–phonon coupling and electron–electron interaction are taken into account. It is found that with increasing of the next-nearest-neighbouring hopping interaction, two kinds of CDW along the main chain appear sequentially. The first CDW is accompanied by perfect dimerization. The second CDW has a period of four lattice sites. The SDW is modulated by the CDW. The interchain coupling causes the transfers of charge density and spin density between the main chain and side radicals, and reduces the critical next-nearest-neighbouring hopping at which the second CDW appears.

1. Introduction

Since organic conductors have been discovered, the possibility of the existence of organic ferromagnetic materials has attracted considerable attention [1–4]. Several research groups in the world have successfully synthesized several organic ferromagnets, such as *m*-PDPC [5] and *p*-NPNN [6]. Various structures have been proposed as possible organic polymer ferromagnets [7–9]. Because the design of the new class of ferromagnetic materials is based on organic molecules rather than metallic or ionic lattices, the mechanism of the organic ferromagnets has not been known clearly.

There are several theoretical model to describe organic ferromagnets. McConnel [10] first proposed to produce intermolecular ferromagnetic interactions in organic molecules in 1963. Ovchinnikov and Spector [11] proposed a simplified structure (shown in figure 1) for an organic ferromagnet. The main zigzag chain consists of π-conjugated carbon atoms, and R is a kind of side radical containing an unpaired electron. They treated the π-electrons along the main chain as an antiferromagnetic spin chain, and assumed that there exists an antiferromagnetic correlation between the π-electron spin and the residual spin of the side radical. Recently, Fang *et al* [12, 13] proposed a theoretical model to deal with the strong electron–electron interaction, the electron–phonon coupling and the antiferromagnetic correlation between itinerant π-electrons and the localized unpaired electrons at the side radical in this organic ferromagnet. They obtained a ferromagnetic ground state, in which a parallel spin arrangement of the unpaired electrons at side free radicals can be gained

0953-8984/98/061371+09$19.50

and there exists an antiferromagnetic spin density wave along the main chain. Fang *et al* [14] also discussed the situation in which the unpaired electrons at side radicals can hop between the main chain and the side radicals. They obtained a ferromagnetic ground state with high spin. However, in these previous works, the system was treated as an isolated chain. Although most organic polymers have a linear chain structure, in some situations, interchain interaction can have a significant effect. Considering the interchain interaction, we have proposed a theoretical model for the quasi-one-dimensional organic ferromagnets [15]. We found that energy levels of split off with respect to different chains. Different configurations of interchain coupling result in transfer of spin density between the main chain and side radical, and appropriate coupling strength stabilizes the high-spin ground state. As a completion of the above work, in this paper, we will consider the next-nearest-neighbouring hopping interactions of π-electrons and side radicals, which can have a considerable size due to the zigzag structure of the main chain and the short C–C bond length. We find that with increasing of the next-nearest-neighbouring hopping interaction, two kinds of CDW along the main chain appear sequentially. The first CDW is accompanied by perfect dimerization. The second CDW has a period of four lattice sites. The SDW is modulated by the CDW. In section 2, we will give the theoretical model and numerical method. Results and discussions will be given in section 3.

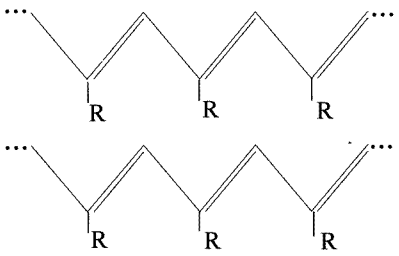

Figure 1. Two neighbouring chains of a quasi-one-dimensional organic ferromagnet.

2. The theoretical model and computational method

We consider two neighbouring coupled chains shown in figure 1. Based on the discussion in section 1, the Hamiltonian exploited in our study can be written as:

$$H = H_1 + H_2 + H' \tag{1}$$

$$\begin{aligned} H_1 = &-\sum_{jl\sigma}[t_0 + \gamma(u_{jl} - u_{jl+1})](c^+_{j1l\sigma}c_{j1l+1\sigma} + \text{HC}) \\ &-\sum_{jl\sigma}[t' + \gamma'(u_{jl} - u_{jl+2})](c^+_{j1l\sigma}c_{j1l+2\sigma} + \text{HC}) - \sum_{jl\sigma}(T_1 c^+_{j1l\sigma}c_{j2l\sigma}\delta_l + \text{HC}) \\ &+\frac{\kappa}{2}\sum_{jl}(u_{jl} - u_{jl+2})^2 - \sum_{jl\sigma}T'_1(c^+_{j1l+1\sigma}c_{j2l\sigma}\delta_l + c^+_{j1l-1\sigma}c_{j2l\sigma}\delta_l + \text{HC}) \end{aligned} \tag{2}$$

$$H_2 = U\sum_{jl}(n_{j1l\alpha}n_{j1l\beta} + n_{j2l\alpha}n_{j2l\beta}\delta_l) \tag{3}$$

$$H' = -\sum_{l\sigma}[T_2(1-\delta_l) + T_3\delta_l](c^+_{11l\sigma}c_{21l\sigma} + \text{HC}) - T_4\sum_{l\sigma}(c^+_{12l\sigma}c_{22l\sigma}\delta_l + \text{HC}). \tag{4}$$

The first term H_1 describes the interchain hoppings of the π-electrons on each main chain and unpaired electrons at side radicals, the electron–phonon interaction and the distortion of the lattice, where $c^+_{jil\sigma}$ ($c_{jil\sigma}$) denotes the creation (annihilation) operator of a π-electron ($i = 1$) along each main chain or an unpaired electron ($i = 2$) at a side radical with spin σ on the ith site in the jth chain, t_0 (t') is the nearest- (next-nearest-) neighbouring hopping integral of the π-electron along each main chain when there is no dimerization, T_1 (T'_1) is the nearest- (next-nearest-) neighbouring hopping integral between a π-electron on the main chain and an unpaired electron at side radical, γ (γ') is the electron–phonon coupling constant, u_{jl} is the displacement of the lth site on the jth main chain, κ is the elastic constant of the lattice. We assume that the side radicals connect with the even carbon atoms, then $\delta_l = 1$ for an even site and $\delta_l = 0$ for an odd site. The second term H_2 describes the Hubbard electron–electron repulsions of π-electrons. $n_{jil\sigma} = c^+_{jil\sigma}c_{jil\sigma}$ ($\sigma = \alpha, \beta$) where α and β denote up and down spin respectively. H' describes the interchain interaction, where T_2 (T_3) is the interchain electron transfer from the odd site (the even site) in the first chain to the corresponding odd site (even site), T_4 is the interchain hopping integral from the side radical in the first chain to the corresponding side radical in the second chain.

It is convenient to cast all quantities into dimensionless form as:

$$h = \frac{H}{t_0} \qquad u = \frac{U}{t_0} \qquad t_i = \frac{T_i}{t_0} \qquad (i = 1, 2, 3, 4)$$
$$\lambda = \frac{2\gamma^2}{t_0\pi\kappa} \qquad y_{jl} = (u_{jl} - u_{jl+1})\gamma/t_0. \tag{5}$$

In order to simplify the Hamiltonian H in equation (1), we select the parameter $\rho = t'/t_0 = T'_1/t_0 = \gamma'/\gamma$, so the Hamiltonian h becomes:

$$h = h_e + h' \tag{6}$$

$$\begin{aligned} h_e = &-\sum_{jl\sigma}[1 + y_{jl}](c^+_{j1l\sigma}c_{j1l+1\sigma} + \text{HC}) - \sum_{jl\sigma}(t_1 c^+_{j1l\sigma}c_{j2l\sigma}\delta_l + \text{HC}) \\ &-\rho\sum_{jl\sigma}[(1 + y_{jl} + y_{jl+1})c^+_{j1l\sigma}c_{j1l+2\sigma} + (c^+_{j1l+1\sigma} + c^+_{j1l-1\sigma})c_{j2l\sigma}\delta_l + \text{HC}] \\ &+u\sum_{jl}(n_{j1l\alpha}n_{j1l\beta} + n_{j2l\alpha}n_{j2l\beta}\delta_l) - \sum_{l\sigma}(t_4 c^+_{12l\sigma}c_{22l\sigma}\delta_l + \text{HC}) \\ &-\sum_{l\sigma}[t_2(1 - \delta_l) + t_3\delta_l](c^+_{11l\sigma}c_{21l\sigma} + \text{HC}) \end{aligned} \tag{7}$$

$$h' = \frac{1}{\pi\lambda}\sum_{jl} y^2_{jl} \tag{8}$$

where h_e is the electronic part of the Hamiltonian, and h' describes the elastic energy of the lattice.

Using a self-consistent iterative method [12, 15], we can numerically solve the Schrödinger equation,

$$h_e\sum_{jil\sigma} z^\sigma_{\mu jil}c^+_{jil\sigma}|0\rangle = \varepsilon_\mu\sum_{jil\sigma} z^\sigma_{\mu jil}c^+_{jil\sigma}|0\rangle \tag{9}$$

where $|0\rangle$ is the true electron vacuum state, ε_μ denotes the μth eigenvector of the Hamiltonian, $Z^\sigma_{\mu jil}$ is the expansion coefficient.

To solve the equation (9), we use the mean-field approximation to divide $n_{jil\sigma}$:

$$n_{jil\sigma} = \langle n_{jil\sigma}\rangle + \Delta n_{jil\sigma} \tag{10}$$

where $\langle\cdots\rangle = \langle G|\cdots|G\rangle$ is the average with respect to the ground state $|G\rangle$, $n_{jil\sigma}$ is fluctuation from the average value. Then we can obtain the following self-consistent iterative equations:

$$\begin{aligned}-[1+y_{jl}]Z^{\sigma}_{\mu j1l+1} - [1+y_{jl-1}]Z^{\sigma}_{\mu j1l-1} - \rho(Z^{\sigma}_{\mu j2l-1}\delta_{l-1} + Z^{\sigma}_{\mu j2l+1}\delta_{1+l}) + u\langle n_{j1l\bar{\sigma}}\rangle Z^{\sigma}_{\mu j1l} \\ -t_1\delta_l Z^{\sigma}_{\mu j2l} - \rho(1+y_{jl}+y_{jl+1})Z^{\sigma}_{\mu j1l+2} - \rho(1+y_{jl-2}+y_{jl-1})Z^{\sigma}_{\mu j1l-2} \\ -[t_2(1-\delta_1)+t_3\delta_l](Z^{\sigma}_{\mu 21l}\delta_{j1} + Z^{\sigma}_{\mu 11l}\delta_{j2}) = \varepsilon^{\sigma}_{\mu} Z^{\sigma}_{\mu j1l} \qquad (j=1,2) \end{aligned} \tag{11}$$

$$\begin{aligned}u\langle n_{j2l\bar{\sigma}}\rangle Z^{\sigma}_{\mu j2l}\delta_l - t_1 Z^{\sigma}_{\mu j1l}\delta_l - t_4(Z^{\sigma}_{\mu 22l}\delta_{j1} + Z^{\sigma}_{\mu 12l}\delta_{j2})\delta_l - \rho(Z^{\sigma}_{\mu j1l-1} + Z^{\sigma}_{\mu j1l+1})\delta_l \\ = \varepsilon^{\sigma}_{\mu} Z^{\sigma}_{\mu 2l} \qquad (j=1,2)\end{aligned} \tag{12}$$

$$\begin{aligned}y_{jl} = \pi\lambda \sum_{\substack{\mu\sigma \\ (occ)}} [Z^{\sigma}_{\mu j1l} Z^{\sigma}_{\mu j1l+1} + \rho(Z^{\sigma}_{\mu j1l+2} Z^{\sigma}_{\mu j1l} + Z^{\sigma}_{\mu j1l-1} Z^{\sigma}_{\mu j1l+1})] \\ + \frac{\pi\lambda}{N} \sum_{l} \sum_{\substack{\mu\sigma \\ (occ)}} [Z^{\sigma}_{\mu j1l} Z^{\sigma}_{\mu j1l+1} + \rho(Z^{\sigma}_{\mu j1l+2} Z^{\sigma}_{\mu j1l} + Z^{\sigma}_{\mu j1l-1} Z^{\sigma}_{\mu j1l+1})].\end{aligned} \tag{13}$$

Here, $\bar{\sigma} = \alpha\delta_{\beta\sigma} + \beta\delta_{\alpha\sigma}$, the periodic boundary conditions are used, N is the number of sites along each main chain, and (occ) means those states occupied by electrons. The dimerization y_{jl} can be obtained by minimizing the total energy $E(y_{jl})$ of the system with respect to y_{jl}:

$$\begin{aligned}E(y_{jl}) = &-\sum_{jl\sigma}[1+(-1)^l y_{jl}] \sum_{\substack{\mu \\ (occ)}} (Z^{\sigma *}_{\mu j1l+1} Z^{\sigma}_{\mu j1l} + Z^{\sigma *}_{\mu j1l} Z^{\sigma}_{\mu j1l+1}) \\ &+ \frac{1}{\pi\lambda}\sum_{jl} y^2_{jl} - \rho \sum_{jl\sigma}[1+y_{jl}+y_{jl+1}] \sum_{\substack{\mu \\ (occ)}} (Z^{\sigma *}_{\mu j1l+2} Z^{\sigma}_{\mu j1l} + Z^{\sigma *}_{\mu j1l} Z^{\sigma}_{\mu j1l+2}) \\ &-\rho \sum_{jl\sigma} \sum_{\substack{\mu \\ (occ)}} [(Z^{\sigma *}_{\mu j1l-1} + Z^{\sigma *}_{\mu j1l+l}) Z^{\sigma}_{\mu j2l} + (Z^{\sigma}_{\mu j1l-1} + Z^{\sigma}_{\mu j1l+1}) Z^{\sigma *}_{\mu j2l}] \\ &-t_1 \sum_{jl\sigma} \sum_{\substack{\mu \\ (occ)}} (Z^{\sigma *}_{\mu j1l} Z^{\sigma}_{\mu j2l} + Z^{\sigma *}_{\mu j2l} Z^{\sigma}_{\mu j1l})\delta_l \\ &-t_4 \sum_{l\sigma} \sum_{\substack{\mu \\ (occ)}} (Z^{\sigma *}_{\mu 12l} Z^{\sigma}_{\mu 22l} + Z^{\sigma *}_{\mu 22l} Z^{\sigma}_{\mu 12l}) \\ &-\sum_{l\sigma}[t_2(1-\delta_l)+t_3\delta_l] \sum_{\substack{\mu \\ (occ)}} (Z^{\sigma *}_{\mu 11l} Z^{\sigma}_{\mu 21l} + Z^{\sigma *}_{\mu 21l} Z^{\sigma}_{\mu 11l}) \\ &+u \sum_{jl} \Bigg(\sum_{\substack{\mu\mu' \\ (occ)}} |Z^{\alpha}_{\mu j1l}|^2 |Z^{\beta}_{\mu' j1l}|^2 + \sum_{\substack{\mu\mu' \\ (occ)}} |Z^{\alpha}_{\mu j2l}|^2 |Z^{\beta}_{\mu' j2l}|^2 \delta_l \Bigg).\end{aligned} \tag{14}$$

The distribution of spin density δn_{jil} and charge density $\langle n_{jil}\rangle$ of π-electrons and unpaired electron at side radicals can be obtained self-consistently as:

$$\delta n_{jil} = \frac{1}{2}(\langle n_{jil\alpha}\rangle - \langle n_{jil\beta}\rangle) = \frac{1}{2}\Bigg(\sum_{\substack{\mu \\ (occ)}} |Z^{\alpha}_{\mu jil}|^2 - |Z^{\beta}_{\mu jil}|^2 \Bigg) \tag{15}$$

$$\langle n_{jil}\rangle = \langle n_{jil\alpha}\rangle + \langle n_{jil\beta}\rangle. \tag{16}$$

The starting geometry in the iterative optimization process is usually the one with zero dimerization. The stability of the optimized geometry is always tested by using another

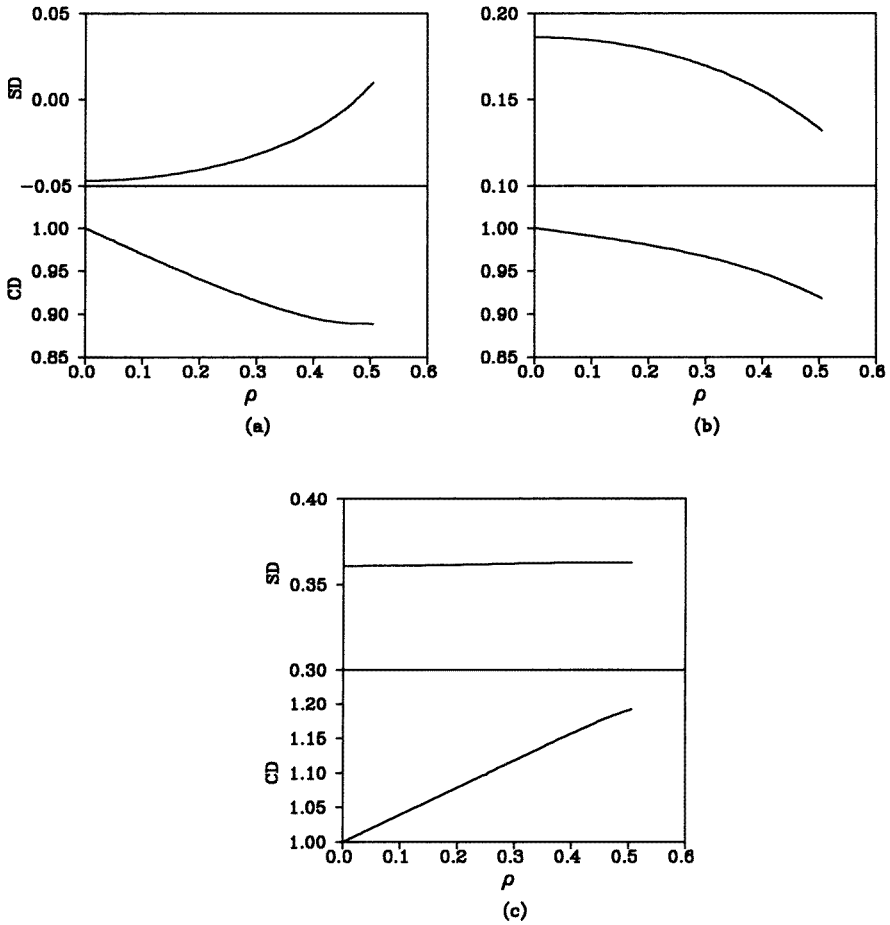

Figure 2. The charge density and spin density at different sites versus the next-nearest-neighbouring hopping integral ρ: (a) at even site on each main chain; (b) at odd site on each main chain; (c) at side radical for $t_2 = t_3 = t_4 = 0$, and $\rho < \rho_c$.

starting configuration and performing the optimization once again. A set of solutions are reached, independent of the starting configuration. The criterion for terminating the optimization is that between two successive iterations, the differences are less than 10^{-7} for the dimerization and spin density.

3. Results and discussions

We consider two neighbouring chains each with 40 carbon atoms and 20 side free radicals (shown in figure 1), and a periodic boundary condition is used. From equations (11) and (12), we know that the eigenvalue equations are asymmetrical with respect to spin owing to the Hubbard electron–electron repulsion. So in this system, the spin degeneracy has been lifted, and we must solve the eigenvalue equations with different spin. In order to study the ground state, we always fill the π-electrons and unpaired electrons at side radicals in the lowest possible levels in every iterative step. Since the investigation on organic ferromagnetic

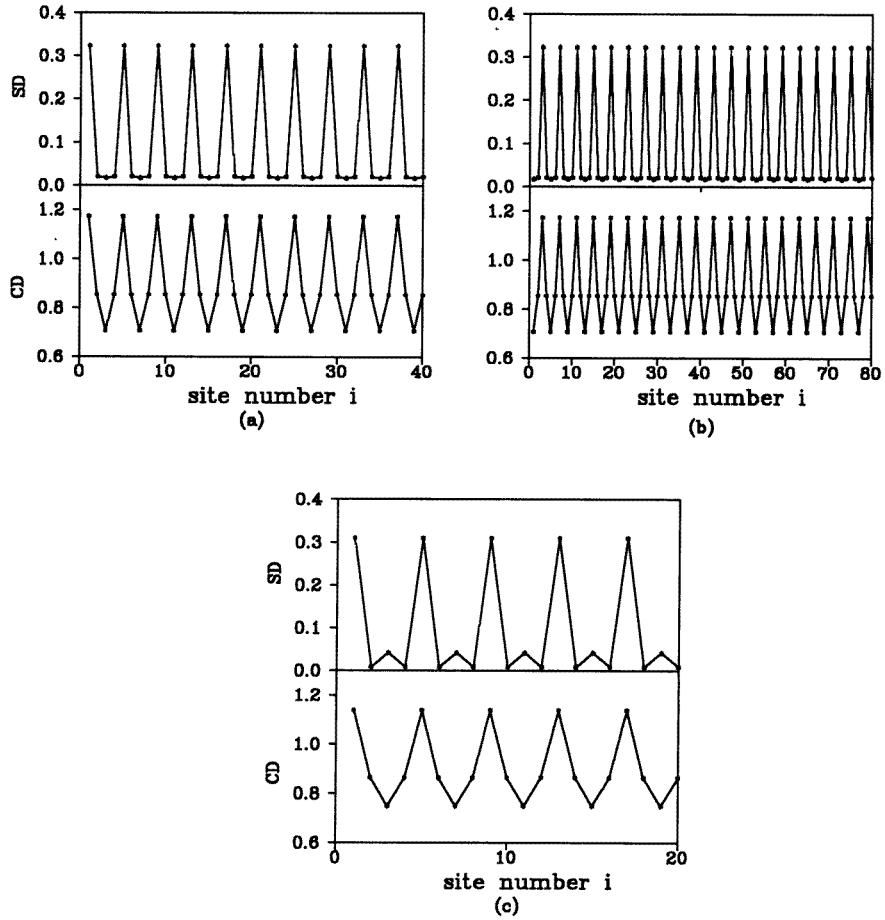

Figure 3. The CDW and SDW along the main chain: for (a) and (b), $\rho = 0.57$, $t_2 = t_3 = t_4 = 0$, the number of carbon atoms along the main chain is $N = 40$ and 80 respectively; for (c), $\rho = 0.48$, $t_2 = t_3 = 0.2$, $t_4 = 0$, $N = 20$.

materials began, experiments concerned with our study have not been reported. As a typical example of studying the mechanism of ferromagnetic interaction in these materials, we just take the e–ph interaction $\lambda = 0.4$, which has the same order as that in polyacetylene [16]. We take the Hubbard e–e correlation $u = 1.0$ under the condition of weak interaction. The hopping term T_1 between the π-electron and R-electron is smaller than that between two neighbouring π-electrons since the R-electron is relatively localized [11, 12]. So we take the parameter $t_1 = 0.9$. We will use the computational results to discuss the effect of the next-nearest-neighbouring hopping integral and interchain coupling on the charge density and spin density.

For an isolated chain in figure 1, considering the Hubbard on-site repulsion and the itineracy of π-electrons along the main chain and the unpaired electron at the side radical, Fang *et al* [14] have obtained a high-spin ground state in which the ferromagnetism is mainly contributed by the side radicals and charge density is distributed uniformly along the main chain and at the side radicals. However, when we consider the interchain coupling and the next-nearest-neighbouring hopping of π-electrons along the main chain and the

unpaired electrons at side radicals, the charge density and spin density will be redistributed inhomogeneously at side radicals and along the main chain. First, we discuss the situation without interchain coupling. The computational result shows that there exists a critical next-nearest-neighbouring hopping integral $\rho_c = 0.53$. When $\rho_c > \rho > 0$, there appears a CDW with a period of two lattice sites along the main chain. The dimerization of the system is perfect. When $\rho > \rho_c$, a new CDW with a period of four lattice sites appears. The system is no longer dimerized perfectly. Figure 2 shows the charge density and spin density at different sites as a function of the next-nearest-neighbouring hopping integral for $\rho < \rho_c$. We find that with increasing of the next-nearest-neighbouring hopping integral ρ, the charge density along the main chain (figure 2(a) and (b)) decreases while the charge density at side radicals (figure 2(c)) increases. This means that ρ makes the electrons transfer from the main chain to the side radicals. As ρ increases, the spin density at the even sites increases while the spin density at the odd site decreases and the spin density at the side radical increases slightly. This means that the spin density transfers mainly along the main chain. Figure 3 shows the CDW and SDW along the main chain for $\rho > \rho_c$. Figure 3(a) and (b) correspond to the situations in which the number of carbon atoms along the main chain is 40 and 80, respectively. We can see clearly that the period of the CDW is four lattice sites for these two situations. The SDW is modulated by the CDW. The further calculation shows that the CDW transition has nothing to do with the number of carbon atoms along the main chain. Comparing figure 2 with figure 3, we also find that for $\rho > \rho_c$, the main chains have a considerable contribution to the high-spin ferromagnetic state.

Then, we discuss the effects of the interchain coupling on the distributions of the charge density and spin density. When we neglect the next-nearest-neighbouring hopping, the ground state is still a high-spin state. The spin density transfers between the main chains and side radicals but the charge density is still distributed uniformly along the main chain and at the side radicals [15]. However, when we add the next-nearest-neighbouring hopping, the transfers of spin density and charge density is quite different, and there still exist two kinds of CDW transition. As the interchain coupling increases, the critical next-nearest-neighbouring hopping ρ_c decreases, but the periods of the CDW are still two lattice sites for $\rho_c > \rho > 0$, and four lattice sites for $\rho > \rho_c$. Figure 3(c) shows the CDW and SDW for $\rho = 0.48$, $\rho_c = 0.44$ when the interchain coupling is $t_2 = t_3 = 0.2$, $t_4 = 0$. Apparently, the period of the CDW and SDW in figure 3(c) is still four lattice sites. Figure 4 shows the charge density and spin density as a function of the interchain coupling t for $\rho = 0.3 < \rho_c$. For curves α, β and γ, the interchain coupling corresponds to $t = t_2$, $t_3 = t_4 = 0$; $t = t_3$, $t_2 = t_4 = 0$ and $t = t_4$, $t_2 = t_3 = 0$, respectively. From curves α in figure 4, we find that with increasing of the interchain hopping t_2 between the corresponding odd sites of two neighbouring chains, the electrons transfer from the side radical and odd site to the even site while the spin density transfers from the odd site to the even site and side radical. Curves β show that as the interchain coupling t_3 between the odd sites increases, the charge density moves from the odd site to the even site and side radical while the spin density transfers slightly from the odd site and side radical to the even site. Curves γ show that with increasing of the interchain coupling t_4 between the side radicals, the charge density transfers from the even site and side radical to the odd site while the spin density transfers from the side radical to the main chain.

In summary, we have studied an interchain coupling model with the next-nearest-neighbouring hopping for an organic ferromagnet. The result shows that with increasing of the next-nearest-neighbouring hopping, there exist two kinds of CDW with the periods of two lattice sites and four lattice sites, respectively. The SDW is modulated by the CDW. The interchain coupling causes the transfers of charge density and spin density between the

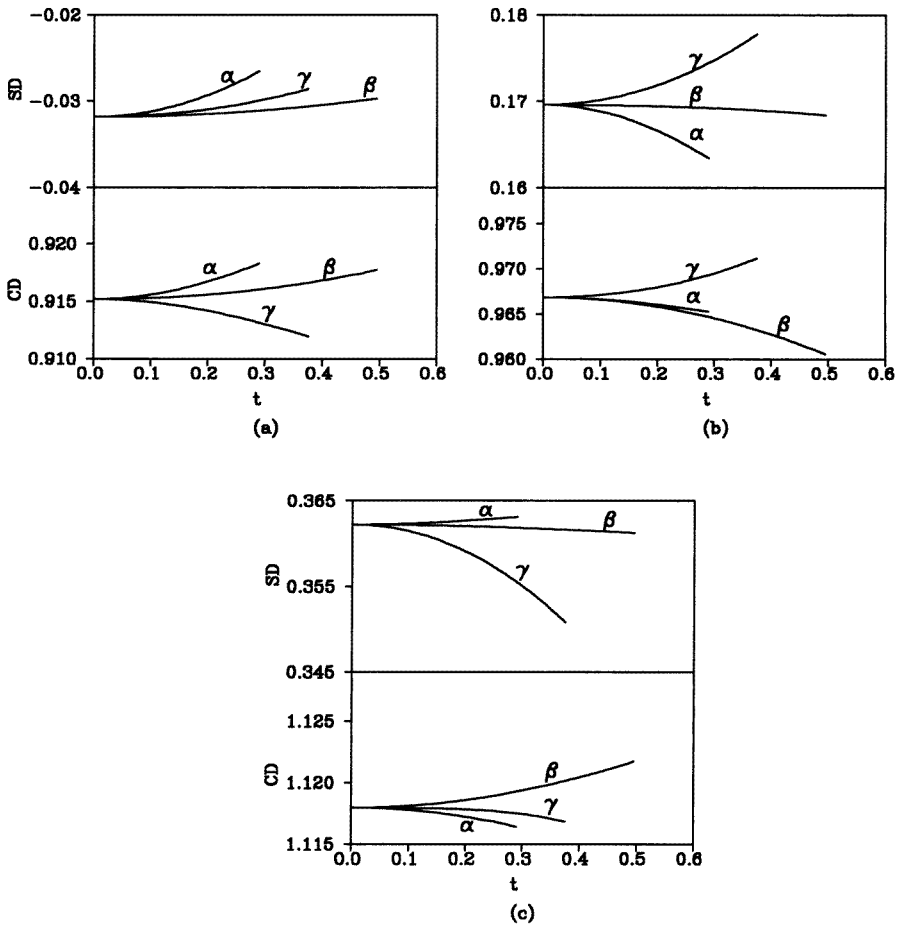

Figure 4. The charge density and spin density at different sites against the interchain coupling t for $\rho = 0.3$: (a) at even site on each main chain; (b) at odd site on each main chain; (c) at side radical. Curve α for $t = t_2$, $t_3 = t_4 = 0$, curve β for $t = t_3$, $t_2 = t_4 = 0$, curve γ for $t = t_4$, $t_2 = t_3 = 0$.

main chain and side radicals, and reduces the critical next-nearest-neighbouring hopping at which the second CDW appears. As is well known, one-dimensional systems, like conducting polymers, charge-transfer solids and transition-metal linear-chain complexes, can show a variety of symmetry-broken ground states like bond ordering wave [17], charge density wave [18, 19], spin density wave [19] and even the superconductor state. These phase transitions originate from the interplay between the electron–electron and electron–phonon interaction. We believe that for the organic ferromagnets the CDW transition will be discovered in future experiments.

Acknowledgments

This work is supported by the National Natural Science Foundation of China and by the Direct Grant for Research from the Research Grants Council of the Hong Kong Government of China.

References

[1] Macedo A M S, dos Santos M C, Coutinho-Filho M D and Macedo C A 1995 *Phys. Rev. Lett.* **74** 1851
[2] Kawamoto T, Shirai M and Suzuki N 1995 *Synth. Met.* **71** 1789
[3] Tanaka K, Ago H and Yamabe T 1995 *Synth. Met.* **72** 225
[4] Nasu K 1986 *Phys. Rev.* B **33** 330
[5] Iwamura H, Sugawra T, Itoh K and Takui T 1985 *Mol. Cryst. Liq. Cryst.* **125** 379
[6] Takahashi M, Turek P, Nakazawa Y, Tamura M, Nozawa K, Shiomi D, Ishikawa M and Kinoshita M 1991 *Phys. Rev. Lett.* **67** 746
[7] Miller J S, Epstein A J and Reiff W M 1988 *Chem. Rev.* **88** 201
[8] Gatteschi D and Sessoli R 1992 *J. Magn. Magn. Mater.* **104–107** 2092
[9] Yoshizawa K, Nakazawa Y, Shiomi D, Nozawa K, Hosokoshi Y, Ishikawa M, Takahashi M and Kimoshita M 1993 *Chem. Phys. Lett.* **202** 483
[10] McConnell H M 1963 *J. Chem. Phys.* **39** 1901
[11] Ovchinnikov A A and Spector V N 1988 *Synth. Met.* **27** B615
[12] Fang Z, Liu Z L and Yao K L 1994 *Phys. Rev.* B **49** 3916
[13] Fang Z, Liu Z L and Yao K L 1995 *Phys. Rev.* B **51** 1304
[14] Fang Z, Liu Z L and Yao K L 1995 *40th Conf. on Magnetism and Magnetic Materials (Philadelphia, PA, 1995)*
[15] Wang W Z, Liu Z L and Yao K L 1997 *Phys. Rev.* B **55** 12 989
[16] Wu C, Sun X and Nasu K 1987 *Phys. Rev. Lett.* **59** 831
[17] Baeriswyl D and Bishop A R 1988 *J. Phys. C: Solid State Phys.* **21** 399
[18] Andrienx A 1979 *Phys. Rev. Lett.* **43** 227
[19] Cava R J 1984 *Phys. Rev. Lett.* **53** 1677